

Fig. 1: Two-hop MIMO AF system model.

convex. However, we show here that the EE-based objective function for the joint SN and RN resource allocation can be approximated by a convex function, and use this property for simplifying this objective function. We then derive explicit formulations of the near-optimal energy-per-bit as well as sub-channels' power and rate for the unconstrained and constrained cases. In turn, we use these expressions for demonstrating that equal aggregate power allocation and allocating power to all the subchannels are the most energy-efficient power allocation in the unconstrained and general scenarios, respectively, at high channel gain-to-noise ratio.

The rest of the paper is organized as follows. Section II describes the two-hop MIMO-AF system in terms of achievable sum-rate, power consumption, and EE formulation based on the energy-per-bit consumption of the system, i.e. Joule-per-bit metric. In Section III, we first prove the existence of a unique global minimum for our EE-based objective function, simplify its formulation and detail how to solve the unconstrained and constrained EE optimization problems in a low-complexity manner, i.e. via one or two unidimensional searches. In Section IV, we first show the reliability and accuracy of our method in comparison with existing approaches as well as provide insights on the energy-efficient asymptotic allocation. As an application, we then compare the EE-optimal performances of two-hop MIMO-AF with MIMO systems. The results indicate that the usage of a relay must improve the quality of the two-hop link by about one order of magnitude in comparison with the direct link for the two-hop MIMO-AF to be more energy efficient than the MIMO system. Our results also show that the extra fixed power consumption induced by transmitting over two hops disadvantage MIMO-AF over MIMO system in terms of EE. However, using a relay can be useful for downsizing the donor cell, which in turn provides EE improvement and overall power consumption reduction at the expense of a lower sum-rate. Conclusions are drawn in Section V.

II. TWO-HOP MIMO AF SYSTEM AND POWER MODELS

A. System model

We consider a two-hop MIMO AF system composed of three nodes, i.e. an SN with n antennas, a nonregenerative RN with q antennas and a destination node (DN) with r antennas, as it is depicted in Fig. 1. The SN transmits data to the DN via the RN over two phases of equal duration, as it has been fully detailed in [15] and [16], such that the aggregate mutual information (over two time slots) of this two-hop MIMO-AF

system can be expressed as

$$I(\mathbf{y}_2; \mathbf{s}) = W \log_2 \left| \mathbf{I}_r + \mathbf{H}_2 \mathbf{G} \mathbf{H}_1 \mathbf{R} \mathbf{R}^\dagger \mathbf{H}_1^\dagger \mathbf{G}^\dagger \mathbf{H}_2^\dagger \right. \\ \left. \times \left(\sigma_2^2 \mathbf{I}_r + \mathbf{H}_2 \mathbf{G} \sigma_1^2 \mathbf{G}^\dagger \mathbf{H}_2^\dagger \right)^{-1} \right|, \quad (1)$$

where the matrices $\mathbf{H}_1 \in \mathbb{C}^{q \times n}$ and $\mathbf{H}_2 \in \mathbb{C}^{r \times q}$ represent the MIMO channels of the SN-RN and RN-DN links, respectively, the matrices $\mathbf{R} \in \mathbb{C}^{n \times n}$ and $\mathbf{G} \in \mathbb{C}^{q \times q}$ are precoding matrices at the SN and RN, respectively, and σ_1^2 and σ_2^2 are the variance of the Gaussian noise vectors $\mathbf{n}_1 \in \mathbb{C}^{q \times 1}$ and $\mathbf{n}_2 \in \mathbb{C}^{r \times 1}$, respectively. In addition, W is the channel bandwidth, \mathbf{I}_x is a $x \times x$ identity matrix, $|\cdot|$ is the matrix determinant, and $(\cdot)^\dagger$ denotes the conjugate transpose.

An optimal precoder is the combination of an optimal precoder structure and an optimal power allocation. The Hadamard determinant theorem [34] establishes that an optimal precoder structure diagonalizes the matrix within the determinant in (1). In the case that the SN-RN link CSI is known at the SN as well as both the SN-RN and RN-DN links' CSI is known at the RN, the SN and RN precoder structures of [15] or [16] have proved to be optimal for maximizing the SE, minimizing the transmit power, and optimizing the EE in [15], [35] and [33], respectively. Applying the SN and RN precoder structures of [15] into (1), the latter simplifies to $I(\mathbf{y}_2; \mathbf{s}) =$

$$R_\Sigma(\mathbf{P}) = W \sum_{m=1}^M \log_2 \left(1 + \frac{p_{2,m} \lambda_{2,m} \sigma_2^{-2} p_{1,m} \lambda_{1,m} \sigma_1^{-2}}{1 + p_{2,m} \lambda_{2,m} \sigma_2^{-2} + p_{1,m} \lambda_{1,m} \sigma_1^{-2}} \right), \quad (2)$$

where $\mathbf{P} = [p_{1,1}, \dots, p_{1,M}, p_{2,1}, \dots, p_{2,M}] \succeq 0$. In addition, $p_{1,m}$ and $p_{2,m}$ are the power elements of \mathbf{P} related to the SN and RN transmit powers, respectively, $\lambda_{i,m}$ denotes the non-zero eigenvalues of \mathbf{H}_i , $i \in \{1, 2\}$, $M = N \triangleq \min \{\text{rk} \{\mathbf{H}_1\}, \text{rk} \{\mathbf{H}_2\}\}$ is the total number of spatial sub-channels and $\text{rk}\{\cdot\}$ is the rank operator. Note that equation (2) is not only valid for the single-carrier two-hop MIMO-AF case but as well as for the multi-carrier scenario [16], where $M = NK$ with K being the number of frequency-flat subchannels. Furthermore, by defining $\mathcal{C}_{1,m} = \log_2(1 + p_{1,m} \lambda_{1,m} \sigma_1^{-2})$ and $\mathcal{C}_{2,m} = \log_2(1 + p_{2,m} \lambda_{2,m} \sigma_2^{-2})$ as the achievable rates over the m -th subchannel of SN-RN and RN-DN links, respectively, equation (2) can be re-expressed as

$$R_\Sigma(\mathcal{C}) = W \sum_{m=1}^M \mathcal{C}_{1,m} + \mathcal{C}_{2,m} - \log_2(2^{\mathcal{C}_{1,m}} + 2^{\mathcal{C}_{2,m}} - 1), \quad (3)$$

with $\mathcal{C} = [\mathcal{C}_{1,1}, \dots, \mathcal{C}_{1,M}, \mathcal{C}_{2,1}, \dots, \mathcal{C}_{2,M}] \succeq 0$.

B. Power consumption model

Even though a base station (BS), a relay, and a user equipment (UE) are different in their architectures and components, it has been shown in [8], [36], [37], [38] and [24], respectively, that their power consumption can be formulated in a similar manner via a linear relation between the consumed and transmit powers, such as

$$P_{\text{in}} = \Delta P + t P_{\text{Ci}}, \quad (4)$$

where Δ and P_{Ci} account for the RF dependent and circuit (fixed) power consumptions, respectively. In addition, t is the

number of transmit antennas and the transmit power, i.e. RF output power, is such that $P \in [0, P^{\max}]$ with P^{\max} being the maximum transmit power. For instance, the total transmit powers at the SN and RN in a two-hop MIMO-AF system are usually bounded as [15]

$$\begin{aligned} 0 \leq P_1(\mathbf{P}) &= \mathbb{E}\{\|\mathbf{R}\mathbf{s}\|_F^2\} \leq P_1^{\max} \quad \text{and} \\ 0 \leq P_2(\mathbf{P}) &= \mathbb{E}\{\|\mathbf{G}\mathbf{y}_1\|_F^2\} \leq P_2^{\max}, \end{aligned} \quad (5)$$

respectively, where $\mathbb{E}\{\cdot\}$ and $\|\cdot\|_F$ stand for the expectation and Frobenius norm. By inserting the optimal SN and RN precoder structures into (5) as well as knowing that $p_{1,m} = \Delta_1^{-1} A_{1,m} (2^{C_{1,m}} - 1)$ and $p_{2,m} = \Delta_2^{-1} A_{2,m} (2^{C_{2,m}} - 1)$, $P_i(\mathbf{P})$ in (5) can be re-expressed as

$$P_i(\mathbf{C}) \triangleq \Delta_i^{-1} \sum_{m=1}^M A_{i,m} (2^{C_{i,m}} - 1), \quad (6)$$

for any $i \in \{1, 2\}$, with $A_{i,m} \triangleq \Delta_i \sigma_i^2 \lambda_{i,m}^{-1}$.

Given the two-phase transmission, the SN will either transmit or be inactive, the RN will either receive or transmit, and the DN will either receive or be inactive. Accordingly, these different types of power consumptions should be reflected in the power model, as in [8] for the BS. Let $P_{\text{Tx}}, P_{\text{Rx}}, P_{\text{Sl}}$ be the transmit, receive and sleep mode powers for any of the nodes, the total power consumed over two time slots by the two-hop MIMO-AF system of Fig. 1 can then be expressed as

$$P_{\Sigma} = (P_{\text{Tx}}^{\text{SN}} + P_{\text{Rx}}^{\text{RN}} + P_{\text{Sl}}^{\text{DN}}) + (P_{\text{Sl}}^{\text{SN}} + P_{\text{Tx}}^{\text{RN}} + P_{\text{Rx}}^{\text{DN}}). \quad (7)$$

In the downlink scenario, the BS and UE are respectively the SN and DN such that $P_{\text{Tx}}^{\text{SN}} = \Delta^{\text{BS}} P_1(\mathbf{C}) + n P_{\text{Ci}}^{\text{BS}}$, $P_{\text{Tx}}^{\text{RN}} = \Delta^{\text{RN}} P_2(\mathbf{C}) + q P_{\text{Ci}}^{\text{RN}}$, $P_{\text{Rx}}^{\text{RN}} = \varsigma q P_{\text{Ci}}^{\text{RN}}$ as well as $P_{\text{Rx}}^{\text{DN}} = \varsigma r P_{\text{Ci}}^{\text{UE}}$ in (7). Hence, based on equation (4)' linear model, P_{Σ} can be re-expressed as

$$P_{\Sigma}(\mathbf{C}) = P_c + \sum_{i=1}^2 \Delta_i P_i(\mathbf{C}), \quad (8)$$

where $\Delta_1 = \Delta^{\text{BS}}$, $\Delta_2 = \Delta^{\text{RN}}$, $P_c = n P_{\text{Ci}}^{\text{BS}} + (1 + \varsigma) q P_{\text{Ci}}^{\text{RN}} + \varsigma r P_{\text{Ci}}^{\text{UE}} + n P_{\text{Sl}}^{\text{BS}} + r P_{\text{Sl}}^{\text{UE}}$, and ς denotes the ratio between transmission and reception overhead powers with $0 \leq \varsigma \leq 1$. Intuitively, receiving consumes less overhead power than transmitting. Similarly, $P_{\Sigma}(\mathbf{C})$ can be obtained as in (8) for the uplink but where the BS and UE are the DN and SN, respectively.

C. EE formulation

The existence of a trade-off between EE and SE implies that EE and SE cannot be optimized separately. Thus, in order to optimize this trade-off, one has first to explicitly formulate it as an objective function. In theory, the EE-SE trade-off of a point-to-point communication system consuming a total power of P_{Σ} Watt for achieving a total rate of R_{Σ} bit/s over a bandwidth W (Hz) can be formulated as [39]

$$\frac{E_b}{N_0} = \frac{C^{-1}(\mathcal{C})}{\mathcal{C}}, \quad (9)$$

when only the RF power of the transmitter is considered as consumed power, i.e. $P_{\Sigma} = P$, and where E_b (Joule) is the transmitted energy per information bit and N_0 (Joule) is the noise power spectral density. In addition, \mathcal{C} is the channel

capacity per unit bandwidth of the system and $C^{-1}(\mathcal{C})$ is its inverse function such that $C^{-1}(\mathcal{C}) = P/\sigma^2$, with $\sigma^2 = N_0 W$. According to (9), the energy-per-bit consumption, E_b , or EE, $1/E_b$, of the two-hop MIMO-AF system can simply be expressed as the ratio of its total consumed power to its sum-rate, which are given in (8) and (3), respectively, such that

$$E_b(\mathbf{C}) = \frac{P_c + \sum_{i=1}^2 \sum_{m=1}^M A_{i,m} (2^{C_{i,m}} - 1)}{W \sum_{m=1}^M \mathcal{C}_{1,m} + \mathcal{C}_{2,m} - \log_2(2^{C_{1,m}} + 2^{C_{2,m}} - 1)}. \quad (10)$$

III. TWO-HOP MIMO-AF EE OPTIMIZATION

In this section, we first show that E_b in (10) has a unique global minimum and, then, utilize this property for simplifying this $2M$ -variable objective function into a M , $M + 1$ and $M + 2$ -variable functions in the unconstrained, sum-rate, single power and dual power constrained EE optimization problems, respectively. We then show that these joint SN and RN resource optimization problems can be formulated in a similar manner as in the single-hop MIMO scenario. Next, we adapt our method of [27] to the MIMO-AF scenario for further simplifying these problems and solving them in a low-complexity manner; a complexity similar to the classic water-filling algorithm in both the unconstrained and sum-rate constrained cases. In the process, we also obtain explicit formulations of the near-optimal energy-per-bit consumption, subchannels' power and rate for the unconstrained and constrained scenarios.

Proposition 1: The function E_b in (10) has a unique global minimum occurring at \mathbf{C}^* , such that $E_b(\mathbf{C}) > E_b^* = E_b(\mathbf{C} = \mathbf{C}^*)$ for $\mathbf{C} \succeq 0$, $\mathbf{C} \neq \mathbf{C}^*$. See Section A of the Appendix for the detailed proof of this proposition.

Proposition 2: Given that E_b in (10) has a unique global minimum, its formulation simplifies to $E_b(\mathbf{C}) =$

$$\begin{aligned} E_b(\mathbf{C}) &= \left[P_c + \sum_{m=1}^M (A_{1,m} + A_{2,m}) (2^{C_m} - 1) + \left(\sqrt{\frac{\mu_1^*}{\mu_2^*}} + \sqrt{\frac{\mu_2^*}{\mu_1^*}} \right) \right. \\ &\quad \left. \times \sqrt{A_{1,m} A_{2,m}} \sqrt{2^{C_m} (2^{C_m} - 1)} \right] \left(W \sum_{m=1}^M \mathcal{C}_m \right)^{-1}, \end{aligned} \quad (11)$$

in the unconstrained as well as sum-rate and power constrained EE optimization problems when $\mathbf{C} = \mathbf{C}^*$ and where

$$\mathcal{C}_m \triangleq \mathcal{C}_{1,m} + \mathcal{C}_{2,m} - \log_2(2^{C_{1,m}} + 2^{C_{2,m}} - 1). \quad (12)$$

In addition, μ_i^* is the optimal value of μ_i , which is a slack variable used in the power constrained optimization cases; in the unconstrained and sum-rate constrained cases, $\mu_1^* = \mu_2^* = 1$. Thus, the $2M$ -variable function in (10) simplifies into a M , $M + 1$ or $M + 2$ -variable function in (11) when $\mathbf{C} = \mathbf{C}^*$. Note that $\mathcal{C}_{1,m}$ and $\mathcal{C}_{2,m}$ can be expressed as a function of \mathcal{C}_m in (12) such that

$$\mathcal{C}_{i,m} = \log_2 \left(2^{C_m} + \sqrt{\frac{\mu_i^* A_{\bar{i},m}}{\mu_i^* A_{i,m}}} \sqrt{2^{C_m} (2^{C_m} - 1)} \right), \quad (13)$$

where $\bar{i} \triangleq \text{mod}\{i, 2\} + 1$ with $\text{mod}\{\cdot, \cdot\}$ being the modulo operator. See Section B of the Appendix for the detailed proof of this proposition.

Remark 1: Given that $2^x - 1 \leq \sqrt{2^x(2^x - 1)} \leq 2^x$ for any $x \geq 0$, $E_b(\mathbf{C})$ in (11) can be lower and upper bounded as

$$\frac{P_c + \sum_{m=1}^M A_m^{-1} (2^{C_m} - 1)}{W \sum_{m=1}^M C_m} \leq E_b(\mathbf{C}) \leq \frac{2\bar{P}_c - P_c + \sum_{m=1}^M A_m^{-1} (2^{C_m} - 1)}{W \sum_{m=1}^M C_m},$$

where $A_m \triangleq (A_{1,m} + A_{2,m} + (\sqrt{\frac{\mu_1^*}{\mu_2^*}} + \sqrt{\frac{\mu_2^*}{\mu_1^*}}) \sqrt{A_{1,m} A_{2,m}})^{-1}$,

$$\bar{P}_c \triangleq P_c + \frac{1}{2} \left(\sqrt{\frac{\mu_1^*}{\mu_2^*}} + \sqrt{\frac{\mu_2^*}{\mu_1^*}} \right) \sum_{m \in \mathcal{M}^*} \sqrt{A_{1,m} A_{2,m}}, \quad (14)$$

and $\mathcal{M}^* = \{m \in \mathcal{M} | C_m^* > 0\}$ is the optimal set of allocated subchannel indices with $\mathcal{M} = \{1, \dots, M\}$.

Remark 2: Note that the two convex functions lower and upper bounding $E_b(\mathbf{C})$ in (11) are formulated in the same manner than $E_b(\mathbf{C})$ for the MIMO system with CSI [27], i.e.

$$E_b(\mathbf{C}) = \frac{P_0 + \sum_{m=1}^M B_m^{-1} (2^{C_m} - 1)}{W \sum_{m=1}^M C_m}, \quad (15)$$

where $B_m = (\Delta^{\text{BS}} \sigma^2)^{-1} \lambda_m$, $P_0 = n P_{\text{Ci}}^{\text{BS}} + \zeta r P_{\text{Ci}}^{\text{UE}}$ and λ_m is the channel gain for each subchannel. In the two-hop MIMO-AF scenario, A_m acts as an aggregate channel gain, which encompasses both the channel gains of the SN-RN and RN-DN channels for each subchannel, and $P_c \geq P_0$.

Proposition 3: According to (11), the optimal value of $E_b(\mathbf{C})$, i.e. $E_b^* \triangleq E_b(\mathbf{C}^*)$, can be expressed as $E_b^* =$

$$\frac{\ln(2)}{W} 2^{C_m^*} \left[\sum_{i=1}^2 \mu_i^* A_{i,m} + \sqrt{\frac{\mu_1^* \mu_2^* A_{1,m} A_{2,m}}{2^{C_m^*} (2^{C_m^*} - 1)}} (2^{C_m^* + 1} - 1) \right], \quad (16)$$

in the unconstrained as well as constrained scenarios, where C_m^* is the optimal value of C_m for any $m \in \mathcal{M}^*$. The full proof of this proposition is provided in Section C of the Appendix.

Corollary 1: A direct consequence of Proposition 3 is that any C_m^* can be formulated in closed-form as a function of E_b^* and μ_i^* , $i \in \{1, 2\}$, by solving the following cubic equation

$$a_{3,m} (2^{C_m^*})^3 + a_{2,m} (2^{C_m^*})^2 + a_{1,m} (2^{C_m^*}) + a_{0,m} = 0,$$

where

$$\begin{aligned} a_{3,m} &= (\mu_1^* A_{1,m} - \mu_2^* A_{2,m})^2, \\ a_{2,m} &= -(2W E_b^* (\mu_1^* A_{1,m} + \mu_2^* A_{2,m}) / \ln(2) + a_{3,m}), \\ a_{1,m} &= (W E_b^* / \ln(2))^2 - \mu_1^* \mu_2^* A_{1,m} A_{2,m} - a_{2,m} - a_{3,m}, \\ a_{0,m} &= -(W E_b^* / \ln(2))^2. \end{aligned} \quad (17)$$

Consequently, the optimal value of C_m is such that

$$C_m^* = \left[\log_2 \left(-\frac{a_{2,m}}{3a_{3,m}} + \frac{1 + j\sqrt{3}}{6a_{3,m}} \sqrt[3]{\frac{1}{2} \left[\Theta_m + \sqrt{\Theta_m^2 - \Lambda_m} \right]} \right) + \frac{1 - j\sqrt{3}}{6a_{3,m}} \sqrt[3]{\frac{1}{2} \left[\Theta_m - \sqrt{\Theta_m^2 - \Lambda_m} \right]} \right]_+, \quad (18)$$

for any $m \in \mathcal{M}^*$, where $[x]_+ = \max\{x, 0\}$, $\Theta_m = 2a_{2,m}^3 - 9a_{3,m}a_{2,m}a_{1,m} + 27a_{3,m}^2a_{0,m}$ and $\Lambda_m = 4(a_{2,m}^2 - 3a_{3,m}a_{1,m})^3$.

Corollary 2: Given that $\sqrt{2^x(2^x - 1)} \approx 2^x - 0.5$, i.e. they differ by less than 1% for $x \geq 2$, $E_b(\mathbf{C})$ in (11), $P_i(\mathbf{C})$ in (6) and E_b^* in (16) can be well-approximated by

$$E_b(\mathbf{C}) \approx \frac{\bar{P}_c + \sum_{m \in \mathcal{M}^*} A_m^{-1} (2^{C_m} - 1)}{W \sum_{m \in \mathcal{M}^*} C_m}, \quad (19a)$$

$$P_i(\mathbf{C}) \approx \tilde{P}_i(\mathbf{C}) = \Delta_i^{-1} \sum_{m \in \mathcal{M}^*} \left(A_{i,m} + \sqrt{\frac{\mu_i^*}{\mu_i^*}} \sqrt{A_{1,m} A_{2,m}} \right) \times \left(2^{C_m} - \frac{1}{2} \right) - \frac{A_{i,m}}{2} \quad \text{and} \quad (19b)$$

$$E_b^* \approx \tilde{E}_b^* = E_b(\tilde{\mathbf{C}}^*) = \ln(2) W^{-1} \hat{A}_m^{-1} 2^{\tilde{C}_m^*}, \quad (19c)$$

respectively, where

$$\hat{A}_m \triangleq (\sqrt{\mu_1^* A_{1,m}} + \sqrt{\mu_2^* A_{2,m}})^{-2} \quad (20)$$

in (19c). Assuming that subchannel l and m are active, equation (19c) yields the following relation between \tilde{C}_l^* and any \tilde{C}_m^* such that, for any $(l, m) \in \mathcal{M}^{*2}$,

$$\tilde{C}_l^* = \tilde{C}_m^* + \log_2 (\hat{A}_m^{-1} \hat{A}_l). \quad (21)$$

A. Unconstrained EE Optimization

In the unconstrained scenario, the EE-based joint optimization problem is such that

$$\min_{\mathbf{C}} E_b(\mathbf{C}) \quad \text{s.t.} \quad \mathbf{C} \geq 0, \quad (22)$$

with $\mu_1^* = \mu_2^* = 1$ in $E_b(\mathbf{C})$ in (11) and $\hat{A}_m = A_m = (\sqrt{A_{1,m}} + \sqrt{A_{2,m}})^{-2}$ in (20). Knowing that (11) is approximately equal to (19a), $E_b(\mathbf{C}^*)$ becomes a single variable function which can be approximated as

$$E_b^* \approx \frac{M^* A_m^{-1} 2^{\tilde{C}_m^*} - \sum_{l \in \mathcal{M}^*} A_l^{-1} + \bar{P}_c}{W \left[M^* (\tilde{C}_m^* - \log_2(A_m)) + \sum_{l \in \mathcal{M}^*} \log_2(A_l) \right]}, \quad (23)$$

by inserting (21) into (19a), where M^* is the optimal number of allocated subchannels ($1 \leq M^* \leq M$) and $\bar{P}_c = P_c + \sum_{l \in \mathcal{M}^*} \sqrt{A_{1,l} A_{2,l}}$ according to (14). Next, by inserting (21) into (19c) and then substituting the left side of (23) with the right side of (19c), we can derive an approximation of C_m^* in closed-form as $C_m^* \approx$

$$\tilde{C}_m^* = \frac{1}{\ln(2)} \left[W_0 \left(\frac{\bar{P}_c - \sum_{l \in \mathcal{M}^*} A_l^{-1}}{M^* e^1 (\prod_{l \in \mathcal{M}^*} A_l)^{-\frac{1}{M^*}}} \right) + 1 \right] - \frac{\sum_{l \in \mathcal{M}^*} \log_2(A_l)}{M^*} + \log_2(A_m), \quad (24)$$

for any $m \in \mathcal{M}^*$, and $\tilde{C}_m^* = 0$ otherwise. In addition, W_0 denotes the real branch of the Lambert function [40]. Similarly to the MIMO case in [27], the value of \tilde{E}_b^* can then be obtained by applying a simple binary-search type of algorithm on M^* , i.e. by finding the number of allocated subchannels that minimizes \tilde{E}_b^* . Note that this process is EE-optimal in the MIMO case but only suboptimal in the MIMO-AF case since (19c) and (23) are only approximations of E_b^* . In order to refine the process and obtain near-optimal C_m^* and E_b^* values, we can use Corollary 1. Indeed, we can refine \tilde{C}_m^* by inserting \tilde{E}_b^* into (17) and (18) and, then, refine \tilde{E}_b^* by inserting the updated \tilde{C}_m^* into (11), as it is summarized in Algorithm 1.

Algorithm 1 Unconstrained optimization

```

1: function UNC( $U, W, P_c, \mu_i^*, A_{i,m}$ )
2:   Compute  $\tilde{\mathcal{C}}_m^*$  in (24) for any  $m \in \{1, U\}$ ;
3:   Obtain  $\tilde{E}_b^* = E_b(\tilde{\mathcal{C}}^*)$  by inserting  $\tilde{\mathcal{C}}_m^*$  into (11);
4:   Refine  $\tilde{\mathcal{C}}_m^*$  by inserting  $\tilde{E}_b^*$  into (17) and (18);
5:   Refine  $\tilde{E}_b^*$  by inserting  $\tilde{\mathcal{C}}_m^*$  into (11);
6:   return  $\tilde{\mathcal{C}}_m^*$  and  $\tilde{E}_b^*$ .
7: end function

8: Inputs:  $M, W, P_c$  and  $A_{i,m}$  for  $i \in \{1, 2\}$  and  $m \in \mathcal{M}$ ;
9: Set  $U = M$  and  $\mu_1^* = \mu_2^* = 1$ ;
10: while  $e^{\frac{A_U}{U}(P_c - \sum_{l=1}^U A_l^{-1} - \sqrt{A_{1,l}A_{2,l}})} < \frac{(\prod_{l=1}^U A_l)^{\frac{1}{U}}}{A_U e^1}$  do  $U = U - 1$ ;
11: Obtain  $M^* \in \{1, U\}$ ,  $\tilde{\mathcal{C}}_m^*$  and  $\tilde{E}_b^*$  via a binary-search on UNC;
12: Outputs:  $\tilde{\mathcal{C}}_m^*$  and  $\tilde{E}_b^*$ .

```

Algorithm 2 Sum-rate constrained optimization

```

1: function SRC( $U, W, P_c, R_{\min}, \mu_i^*, A_{i,m}$ )
2:   Compute  $\tilde{\mathcal{C}}_m^*$  in (27) for any  $m \in \{1, U\}$ ;
3:   Same as lines 3 and 4 of UNC;
4:   Set  $\tilde{\mathcal{C}}_m^* = \tilde{\mathcal{C}}_m^* R_{\min} / \left(\sum_{l=1}^U \tilde{\mathcal{C}}_l^*\right)$  (Normalization);
5:   Refine  $\tilde{E}_b^*$  by inserting  $\tilde{\mathcal{C}}_m^*$  into (11);
6:   return  $\tilde{\mathcal{C}}_m^*$  and  $\tilde{E}_b^*$ .
7: end function

8: Inputs:  $M, W, P_c, R_{\min}$  and  $A_{i,m}$  for  $i \in \{1, 2\}$  and  $m \in \mathcal{M}$ ;
9: Set  $U = M$  and  $\mu_1^* = \mu_2^* = 1$ ;
10: while  $2^{\frac{R_{\min}}{UW}} < \frac{(\prod_{l=1}^U A_l)^{\frac{1}{U}}}{A_U}$  do  $U = U - 1$ ;
11: Obtain  $M^* \in \{1, U\}$ ,  $\tilde{\mathcal{C}}_m^*$  and  $\tilde{E}_b^*$  via a binary-search on SRC;
12: Outputs:  $\tilde{\mathcal{C}}_m^*$  and  $\tilde{E}_b^*$ .

```

B. Sum-rate Constrained EE Optimization

Assuming an end-to-end sum-rate constraint, i.e. over two-hops, the EE-based joint optimization problem is such that

$$\begin{aligned} \min_{\mathcal{C}} E_b(\mathcal{C}) \\ \text{s.t. } \mathcal{C} \succeq 0, R_{\Sigma}(\mathcal{C}) \geq R_{\min}. \end{aligned} \quad (25)$$

In the case that $R_{\Sigma}(\mathcal{C}) > R_{\min}$ for $\mathcal{C} = \mathcal{C}^*$, the EE-optimal unconstrained solution of (22), which can be obtained via Algorithm 1, is also the solution of (25). Otherwise, when the rate constraint is enforced, i.e. $R_{\Sigma}(\mathcal{C}) = R_{\min}$ in (25), then $E_b(\mathcal{C}) = \frac{P_{\Sigma}(\mathcal{C})}{R_{\min}}$ and, hence, the EE-based optimization problem in (25) reverts to a power minimization problem with the following associated Lagrangian

$$\mathcal{L}(\mathcal{C}, \nu) = P_{\Sigma}(\mathcal{C}) + \nu(R_{\min} - R_{\Sigma}(\mathcal{C})), \quad (26)$$

where ν is a slack variable. As it is explained in Section C of the Appendix, solving $\nabla \mathcal{L}(\mathcal{C}^*, \nu^*) = \mathbf{0}$ yields relation (16) but with ν^* instead of E_b^* in the left side of (16). Therefore, we can use Corollary 1 to formulate \mathcal{C}_m^* as a function of ν^* (by replacing E_b^* with ν^* and setting $\mu_1^* = \mu_2^* = 1$ in (17) and (18)), where ν^* acts as a water-level. Then, we can obtain the optimal ν^* as well as \mathcal{C}_m^* in a low-complexity manner by using a simple water-filling approach such that $R_{\Sigma}(\mathcal{C}(\nu^*)) - R_{\min} = 0$. Alternatively, knowing that (24) simplifies to

$$\tilde{\mathcal{C}}_m^* = \begin{cases} \frac{1}{M^*} \left(\frac{R_{\min}}{W} - \sum_{l \in \mathcal{M}^*} \log_2(A_l) \right) + \log_2(A_m), & \forall m \in \mathcal{M}^* \\ 0, & \text{otherwise} \end{cases} \quad (27)$$

when $R_{\Sigma}(\mathcal{C}) = R_{\min}$, we can use a similar algorithm as in the unconstrained scenario, which is summarized in Algorithm 2.

C. Total Transmit Power Constrained EE Optimization

Considering that the total transmit power at the SN and/or RN is constrained, the EE-based joint problem is given by

$$\begin{aligned} \min_{\mathcal{C}} E_b(\mathcal{C}) \\ \text{s.t. } \mathcal{C} \succeq 0, P_i(\mathcal{C}) \leq P_i^{\max}, i \in \{1, 2\}. \end{aligned} \quad (28)$$

In the case that both $P_1(\mathcal{C}) < P_1^{\max}$ and $P_2(\mathcal{C}) < P_2^{\max}$ for $\mathcal{C} = \mathcal{C}^*$, the EE-optimal unconstrained solution of (22), which can be obtained via Algorithm 1, is also the solution

of (28). Whenever this condition is not met, we design a low-complexity near-optimal algorithm for both the single and dual power constrained cases in Algorithm 3.

1) Single Transmit Power Constrained at the SN or RN:

In the case that the SN or RN transmits at full power, then $P_i(\mathcal{C}) = P_i^{\max}$ ($i = 1$ or 2) in (28) and the Lagrangian associated to the optimization problem in (28) is given by

$$\begin{aligned} \mathcal{L}(\mathcal{C}, \hat{\mu}_i) = [P_c + \Delta_i(1 - \hat{\mu}_i R_{\Sigma}(\mathcal{C}))P_i^{\max} + \Delta_{\bar{i}}P_{\bar{i}}(\mathcal{C}) \\ + \hat{\mu}_i R_{\Sigma}(\mathcal{C})\Delta_i P_i(\mathcal{C})] R_{\Sigma}(\mathcal{C})^{-1}, \end{aligned} \quad (29)$$

where $\hat{\mu}_i$ is a slack variable. Given that $\tilde{P}_i(\mathcal{C}) \approx P_i^{\max}$, we can approximate \mathcal{C}_m^* by inserting (21) into $\tilde{P}_i(\mathcal{C})$ in (19b) as

$$\tilde{\mathcal{C}}_m^* = \left[\log_2 \left(\frac{\Delta_i P_i^{\max} + \sum_{l \in \mathcal{M}^*} A_{i,l} + \frac{(\mu^*)^{\frac{i-\bar{i}}{2}}}{2} \sqrt{A_{1,l}A_{2,l}}}{\sum_{l \in \mathcal{M}^*} \beta_l(\mu^*) \left(A_{i,l} + (\mu^*)^{\frac{i-\bar{i}}{2}} \sqrt{A_{1,l}A_{2,l}} \right)} \right) \right]_+^+, \quad (30)$$

where $\mu^* = \mu_1^*/\mu_2^*$, $\mu_i^* = \hat{\mu}_i^* R_{\Sigma}(\mathcal{C}^*)$, $\forall i \in \{1, 2\}$, and

$$\beta_l(\mu^*) = \hat{A}_m^{-1} \hat{A}_l = \left(\frac{\sqrt{\mu^* A_{1,m}} + \sqrt{A_{2,m}}}{\sqrt{\mu^* A_{1,l}} + \sqrt{A_{2,l}}} \right)^2. \quad (31)$$

Note that $\mu_i^* = 1$ in the single power constrained case. In addition, according to equations (13)/(50) and (48), $\tilde{\mathcal{C}}_{i,m}^*$ relates to $\tilde{\mathcal{C}}_m^*$ and $\tilde{\mathcal{C}}_{i,m}^*$, respectively, as follows

$$\tilde{\mathcal{C}}_{i,m}^* = \log_2 \left(1 + \frac{P_i^{\max}}{P_i(\tilde{\mathcal{C}}^*)} \left(2^{\tilde{\mathcal{C}}_{i,m}^*} - 1 \right) \right) \quad \text{and} \quad (32a)$$

$$\tilde{\mathcal{C}}_{\bar{i},m}^* = \log_2 \left(1 + \sqrt{1 + 4 \frac{\mu_i^* A_{i,m}}{\mu_{\bar{i}}^* A_{\bar{i},m}} 2^{\tilde{\mathcal{C}}_{i,m}^*} \left(2^{\tilde{\mathcal{C}}_{i,m}^*} - 1 \right)} \right) - 1, \quad (32b)$$

where $\mathcal{C}_{i,m}$ and P_i as a function of \mathcal{C}_m are provided in (13) and (50), respectively. By using (30) in conjunction with (32) and the latter result into (12), we can obtain a robust approximation of $\tilde{\mathcal{C}}_m^*$ solely as a function μ_i^* , as it is indicated in our single power constrained (SPC) function. Then, by inserting the latter into (11), we can express \tilde{E}_b^* solely as a function of M^* and μ_i^* . For a given M^* , μ_i^* can be obtained by using a unidimensional search algorithm on μ_i^* , e.g. Golden section search, Newton-Raphson method, etc. [41]. Knowing that (11)

```

1: function SPC( $U, W, P_c, P_i^{\max}, \Delta_i, \mu_i^*, A_{i,m}$ )
2:   Set  $\iota = \mu_i^*, u = 0, u_{\min} = 1, t = 0$ , and  $\epsilon = 10^{-4}$ ;
3:   while  $|\mu_i^* - u| > \epsilon$  do
4:     Set  $u = \mu_i^*$ ;
5:     Compute  $\tilde{C}_m^*$  in (30) for any  $m \in \{1, U\}$ ;
6:     Compute  $\bar{U} = \sum_{m=1}^U (\tilde{C}_m^* > 0)$ ;
7:     if  $\bar{U} \neq U$  then  $U = \bar{U}, \mu_i^* = \iota, u = \iota, u_{\min} = 1$  and  $t = 0$ ;
8:     Get  $\tilde{C}_{i,c}^*$  and  $\tilde{C}_{i,m}^*$  by inserting  $\tilde{C}_m^*$  into (32),  $m \in \{1, U\}$ ;
9:     Normalize  $\tilde{C}_m^*$  by inserting  $\tilde{C}_{i,c}^*$  and  $\tilde{C}_{i,m}^*$  into (12);
10:    Obtain  $\mu_i^*$  by inserting  $\tilde{C}_m^*$  into (33);
11:    if  $t == 0$  then  $u_{\max} = \max(\mu_i^*, \iota)$  and  $t = 1$ ;
12:    if  $u > \mu_i^*$  then  $u_{\max} = u$  else  $u_{\min} = u$ ;
13:    Set  $\mu_i^* = (u_{\min} + u_{\max})/2$ ;
14:  end while
15:  Obtain  $\tilde{E}_b^*$  by inserting  $\tilde{C}_m^*$  and  $\mu_i^*$  into (11);
16:  return  $\mu_i^*, \tilde{C}_m^*$  and  $\tilde{E}_b^*$ 
17: end function

```

and (16) are equal for μ_i^* and $\mathcal{C} = \mathcal{C}^*$, μ_i^* can also be obtained in closed-form as a function of \mathcal{C}_m^* , such that

$$\mu_i^* = \left(-\frac{b_2}{3b_3} + \sum_{k=1}^2 \frac{1 + j^{2k-1}\sqrt{3}}{6b_3} \sqrt[3]{\frac{1}{2} \left[\Theta + j^{2k}\sqrt{\Theta^2 - \Lambda} \right]} \right)^2, \quad (33)$$

where $\Theta = 2b_2^3 - 9b_3b_2b_1 + 27b_3^2b_0$, $\Lambda = 4(b_2^2 - 3b_3b_1)^3$, $b_0 = -\sum_{m=1}^U \sqrt{A_{1,m}A_{2,m}2^{C_m^*}(2^{C_m^*} - 1)}$, $b_1 = \frac{\ln(2)}{U} \left(\sum_{m=1}^U C_m^* \right) \times \left(\sum_{m=1}^U 2^{C_m^*} A_{i,m} \right) - \left(P_c + \sum_{m=1}^U (A_{1,m} + A_{2,m}) (2^{C_m^*} - 1) \right)$, $b_2 = \frac{\ln(2)}{U} \left(\sum_{m=1}^U C_m^* \right) \left(\sum_{m=1}^U \sqrt{\frac{2^{C_m^*} A_{1,m} A_{2,m}}{(2^{C_m^*} - 1)}} (2^{C_m^* + 1} - 1) \right) + b_0$, $b_3 = \frac{\ln(2)}{U} \left(\sum_{m=1}^U C_m^* \right) \left(\sum_{m=1}^U 2^{C_m^*} A_{i,m} \right)$.

2) Dual Transmit Power Constrained at the SN and RN:

In the case that both the SN and RN transmit at full power, the Lagrangian associated to the EE optimization problem in (28) can be expressed as $\mathcal{L}(\mathcal{C}, \hat{\mu}_1, \hat{\mu}_2) = R_{\Sigma}(\mathcal{C})^{-1} \times$

$$\left(P_c + \sum_{i=1}^2 \Delta_i [(1 - \hat{\mu}_i R_{\Sigma}(\mathcal{C})) P_i^{\max} + \hat{\mu}_i R_{\Sigma}(\mathcal{C}) P_i(\mathcal{C})] \right). \quad (34)$$

This problem is equivalent to optimizing the sum-rate subject to both the SN and RN transmitting at full power. Although, this problem has been investigated in the literature [18], [20] from an SE perspective, we solve it here from an EE perspective. Similar to the single power constraint case, \tilde{C}_m^* can be formulate solely as a function μ^* as in (30). Given that \tilde{C}_m^* must be identical for $i = 1$ and $i = 2$, μ^* can be obtained from (30) by solving a quadratic equation, such that

$$\mu^* = \frac{1}{4} \left(\frac{c_1 c_2 - c_0 c_3}{c_0 c_4 - c_2 c_5} + \sqrt{\left(\frac{c_0 c_3 - c_1 c_2}{c_0 c_4 - c_2 c_5} \right)^2 + 4 \frac{c_1 c_4 - c_3 c_5}{c_0 c_4 - c_2 c_5}} \right)^2, \quad (35)$$

with $c_0 = \Delta_1 P_1^{\max} + \sum_{l=1}^U A_{1,l}$, $c_1 = \Delta_2 P_2^{\max} + \sum_{l=1}^U A_{2,l}$, $c_2 = \sum_{l=1}^U \beta_l(\mu^*) A_{1,l}$, $c_3 = \sum_{l=1}^U \beta_l(\mu^*) A_{2,l}$, $c_4 = \sum_{l=1}^U \beta_l(\mu^*) \sqrt{A_{1,l} A_{2,l}}$ and $c_5 = \sum_{l=1}^U \sqrt{A_{1,l} A_{2,l}}/2$. Next, \tilde{C}_m^* is obtained by inserting μ^* into (30) and, then, refined by using (32a) and (12). Knowing that (11) and (16) are equal for μ_i^* and $\mathcal{C} = \mathcal{C}^*$, μ_2^* can be expressed in closed-form as a

```

1: function DPC( $U, W, P_c, P_i^{\max}, \Delta_i, A_{i,m}$ )
2:   Set  $\mu^* = 1, U = 0, \bar{U} = U$  and  $\epsilon = 10^{-4}$ ;
3:   while  $(U \neq \bar{U}) \& (\bar{U} > 0)$  do
4:      $U = \bar{U}$  and  $u = 0$ ;
5:     while  $|\mu^* - u| > \epsilon$  do
6:       Set  $u = \mu^*$ ;
7:       Compute  $\beta_l(\mu^*)$  in (31) for any  $l \in \{1, U\}$  and  $m = 1$ ;
8:       Obtain  $\mu^*$  by inserting  $\beta_l(\mu^*)$  into (35);
9:     end while
10:    Compute  $\tilde{C}_m^*$  in (30) for either  $i = 1$  or  $2$ ;
11:    Compute  $\bar{U} = \sum_{m=1}^U (\tilde{C}_m^* > 0)$ ;
12:    if  $\bar{U} < 2$  then
13:      Set  $\bar{U} = 1$  and  $\tilde{C}_{i,m}^* = \log_2(1 + A_{i,m}^{-1} \Delta_i P_i^{\max})$ ;
14:    else
15:      Obtain  $\tilde{C}_{i,c}^*$  and  $\tilde{C}_{i,m}^*$  by inserting  $\tilde{C}_m^*$  into (32a);
16:    end if
17:    Normalize  $\tilde{C}_m^*$  by inserting  $\tilde{C}_{i,c}^*$  and  $\tilde{C}_{i,m}^*$  into (12);
18:  end while
19:  Obtain  $\mu_2^* =$  via equation (36) and set  $\mu_1^* = \mu_2^* \mu^*$ ;
20:  Obtain  $\tilde{E}_b^*$  by inserting  $\tilde{C}_m^*$  into (11);
21:  Refine  $\tilde{C}_m^*$  by inserting  $\tilde{E}_b^*, \mu_1^*$  and  $\mu_2^*$  into (17) and (18);
22:  Refine  $\tilde{C}_{i,c}^*$  and  $\tilde{C}_{i,m}^*$  by inserting  $\tilde{C}_m^*$  into (32a);
23:  Normalize  $\tilde{C}_m^*$  by inserting  $\tilde{C}_{i,c}^*$  and  $\tilde{C}_{i,m}^*$  into (12);
24:  Refine  $\tilde{E}_b^*$  by inserting  $\tilde{C}_m^*$  into (11);
25:  return  $\mu_1^*, \mu_2^*, \tilde{C}_m^*$  and  $\tilde{E}_b^*$ 
26: end function

```

Algorithm 3 Power constrained optimization

```

1: Inputs:  $M, W, P_c, P_i^{\max}, \Delta_i, \tilde{C}_m^*$  and  $A_{i,m}, \forall i \in \{1, 2\}, m \in M$ 
2: Compute  $U = \sum_{m=1}^U (\tilde{C}_m^* > 0)$ ;
3: Compute  $P_1(\tilde{\mathcal{C}}^*)$  and  $P_2(\tilde{\mathcal{C}}^*)$  by using (50) for  $\mu_1^* = \mu_2^* = 1$ ;
4: if  $P_1(\tilde{\mathcal{C}}^*) \geq P_1^{\max}$  or  $P_2(\tilde{\mathcal{C}}^*) \geq P_2^{\max}$  then ▷ SPC
5:   if  $\frac{P_1(\tilde{\mathcal{C}}^*)}{P_1^{\max}} > \frac{P_2(\tilde{\mathcal{C}}^*)}{P_2^{\max}}$  then  $i = 1$  else  $i = 2$ ;
6:   Set  $\bar{i} = \text{mod} \{i, 2\} + 1$ ,  $\mu_i^* = \frac{P_i(\tilde{\mathcal{C}}^*)}{P_i^{\max}}$  and  $\mu_{\bar{i}}^* = 1$ ;
7:   Obtain  $M^* \in \{1, U\}$ ,  $\tilde{C}_m^*$  and  $\tilde{E}_b^*$  via a binary-search on SPC;
8:   Compute  $P_{\bar{i}}(\tilde{\mathcal{C}}^*)$  by using (50) knowing  $\mu_i^*$  and  $\mu_{\bar{i}}^* = 1$ ;
9:   if  $P_{\bar{i}}(\tilde{\mathcal{C}}^*) \geq P_{\bar{i}}^{\max}$  then ▷ Dual Power Constraint
10:    Obtain  $M^*, \tilde{C}_m^*$  and  $\tilde{E}_b^*$  via a binary-search on DPC;
11:   end if
12: end if
13: Outputs:  $\mu_1^*, \mu_2^*, \tilde{C}_m^*$  and  $\tilde{E}_b^*$ .

```

function of \mathcal{C}_m^* and μ^* , such that $\mu_2^* = \frac{UW}{\ln(2)} E_b(\mathcal{C}^*) \times$

$$\left[\sum_{m=1}^U 2^{C_m^*} \left(\mu^* A_{1,m} + A_{2,m} + \sqrt{\frac{\mu^* A_{1,m} A_{2,m}}{2^{C_m^*} (2^{C_m^*} - 1)}} (2^{C_m^* + 1} - 1) \right) \right]^{-1}, \quad (36)$$

where $E_b(\mathcal{C})$ is given in (11) for $M = U$. More details about the dual power constrained (DPC) function are given above.

D. Energy-efficient MIMO-AF procedure

The unconstrained EE optimization problem becomes either a rate maximization or power minimization problem when either both the SN and RN transmit at full power or the two-hop link cannot support a target rate, respectively. Thus, EE optimization is a generalization of both SE and power optimizations such that enforcing rate or power constraints on EE provides either a power or SE-optimal solution, which, however, is suboptimal in terms of EE. The sole EE-optimal

TABLE I: Power parameter values

Parameters	Δ	P_{C_1} (W)	P_{S_1} (W)	P^{\max} (W)
MaBS [8]	4.7	130	75	20
MiBS [8]	2.6	56	39	6.3
RN [38]	6.3	6.45	—	1
UE [24]	—	0.1	0.02	—

solution is the optimal unconstrained EE solution. Consequently, Algorithm 1 must first be used to find the optimal unconstrained energy-efficient joint SN and RN resource allocation. If $W \sum_{m \in \mathcal{M}^*} \tilde{C}_m^* \leq R_{\min}$, then the allocation is refined by using Algorithm 2. Similarly, if $P_1(\tilde{\mathcal{C}}^*) \geq P_1^{\max}$ or $P_2(\tilde{\mathcal{C}}^*) \geq P_2^{\max}$, then the allocation is refined by using Algorithm 3. At the end of the algorithm near-optimal values of $C_{1,m}^*$ and $C_{2,m}^*$ are obtained by inserting μ_1^* , μ_2^* and \tilde{C}_m^* into (13). Whereas, near-optimal values of $p_{1,m}^*$ and $p_{2,m}^*$ are obtained by inserting $C_{1,m}^*$ and $C_{2,m}^*$ into $p_{1,m} = \Delta_1^{-1} A_{1,m} (2^{C_{1,m}^*} - 1)$ and $p_{2,m} = \Delta_2^{-1} A_{2,m} (2^{C_{2,m}^*} - 1)$, respectively. Note that as in [15], [33], we assume that the eigenvalues $\lambda_{1,m}$ and $\lambda_{2,m}$ are sorted in descending order for each link prior to using our algorithms.

E. Algorithms' accuracy results

In order to demonstrate the reliability of our algorithms, i.e. Algorithms 1, 2 and 3, for jointly optimizing the SN and RN resource allocation in an energy-efficient manner, we compare their results, averaged over 1000 runs, against the holistic results of [33] and those of the Matlab “fmincon” function in Figs. 2 and 3. Given that E_b is quasiconvex, one can solve the optimization problems in (22), (25) and (28) via usual convex optimization tools such as the Matlab “fmincon” function.

We depict in Figs. 2 and 3, the unconstrained and single transmit power, dual transmit power as well as sum-rate constrained results, respectively, as a function of the RN and DN noise powers for various numbers of subchannels, power and rate constraint values. These figures are plotted by assuming a MIMO Rayleigh fading channel between each node and using the values of Table I, when considering a macro BS (MaBS) at the SN, for setting the various power parameters of Section II-B. Moreover, $W = 1$ as well as $\zeta = 0.5$, and $\sigma_i^2 = 0$ dB in Fig. 3. The results clearly show the tight match between our algorithm results and the “fmincon” function results for both the unconstrained as well as constrained scenarios, and regardless of the numbers of subchannels and constraint values. In turn, it graphically confirms the great accuracy and reliability of our low-complexity energy-efficient joint SN and RN resource allocation method for the two-hop MIMO-AF system. Moreover, our algorithms outperform the holistic approach in [33] for $R_{\min} = 20$ bit/s and provide similar results to [33] in the other settings.

IV. INSIGHTS, APPLICATIONS AND RESULTS

A. EE MIMO-AF Optimization insights

Let us define $p_m \triangleq A_m^{-1} (2^{C_m} - 1)$ as the per-subchannel aggregate transmit power such that $2^{C_m} = A_m p_m + 1$. The

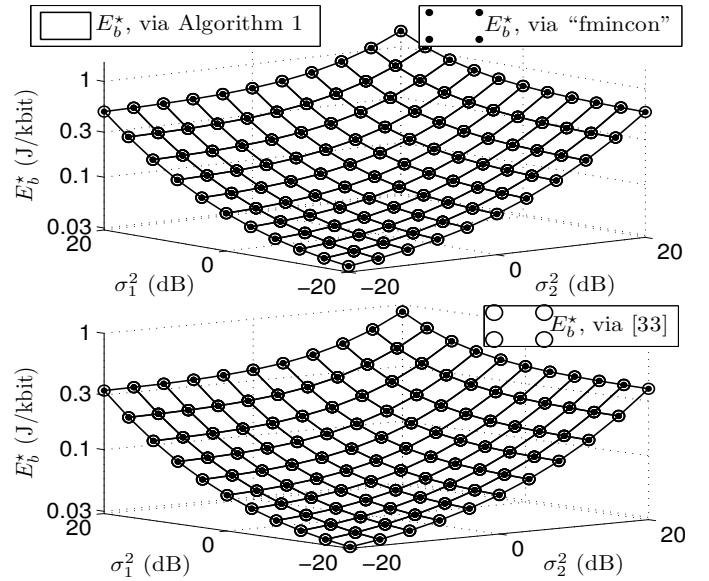


Fig. 2: Comparison of the optimal energy-per-bit consumption obtained via our Algorithm 1, “fmincon” and the method in [33] for the unconstrained scenario with $K = 1$ & $N = 4$ (upper graph) as well as $K = 1$ & $N = 16$ (lower graph).

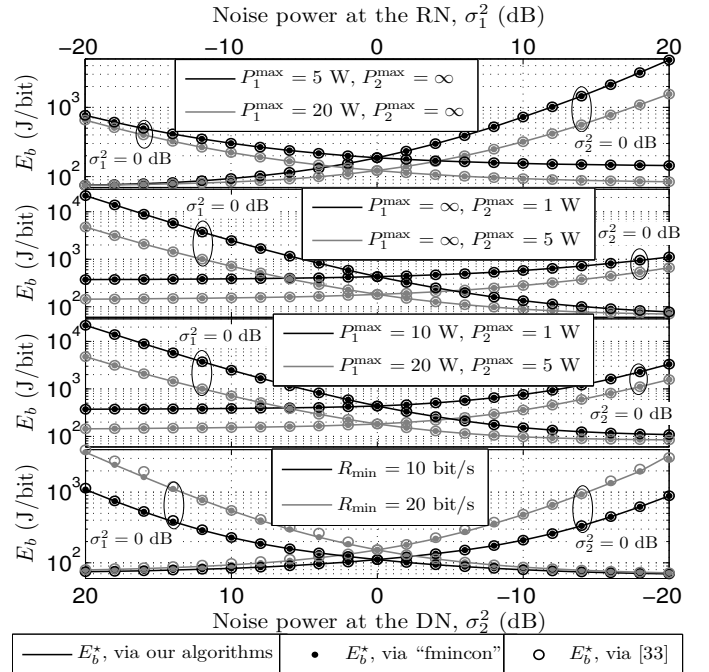


Fig. 3: Comparison of the optimal energy-per-bit consumption obtained via our Algorithms 2/3, “fmincon” and the method in [33] for the transmit power or rate constrained scenario with $K = 1$ & $N = 4$.

optimal per-subchannel aggregate transmit power can then be approximated as

$$p_m^* \approx \tilde{p}_m^* = A_m^{-1} \left[\hat{A}_m W E_b^* / \ln(2) - 1 \right]_+ \quad (37)$$

by substituting $2^{\tilde{C}_m^*}$ with $A_m \tilde{p}_m^* + 1$ in (19c). Given that \hat{A}_m increases as both $A_{1,m}$ and $A_{2,m}$ decrease,

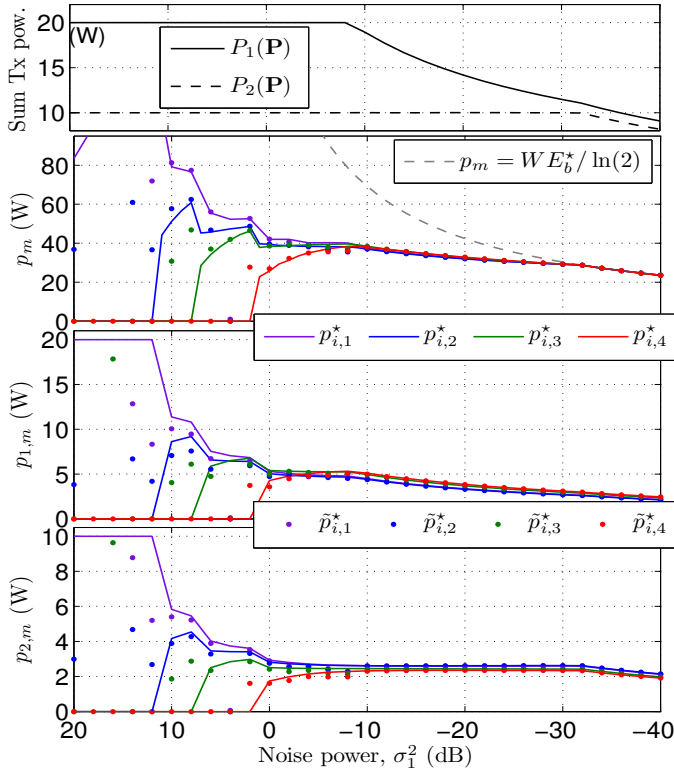


Fig. 4: EE-optimal total transmit powers at the SN as well as RN, and EE-optimal SN and RN per-subchannel transmit and aggregate transmit powers.

(37), asymptotic expressions of the EE-optimal SN and RN per-subchannel transmit powers can be formulated as

$$\tilde{p}_{i,m}^* = \frac{\sigma_i^2 [\hat{A}_m W E_b^* / \ln(2) - 1]_+}{\lambda_{i,m}} \left(1 + \sqrt{\frac{\mu_i^* A_{i,m}^-}{\mu_i^* A_{i,m}^+}} \right). \quad (38)$$

In order to verify our previous premises, we depict in Fig. 4 the total transmit powers at the SN as well as RN, and the EE-optimal SN and RN per-subchannel transmit and aggregate transmit powers as a function of the noise power $\sigma_1^2 = \sigma_2^2$. We consider $M = 4$ subchannels for each link with the following gain values $\lambda_1 = [5.1, 3.7, 2.1, 0.9]$ and $\lambda_2 = [3.9, 2.7, 2.2, 1.1]$. We also set $W = 1$, $P_1^{\max} = 20$ W, $P_2^{\max} = 10$ W, and the other power parameter values according to Table I. It can be seen in the first subplot that at high noise power, the optimal total transmit powers at both SN and RN are constrained. As the noise power decreases (as A_m increases), as the optimal total transmit powers become progressively unconstrained, from $\sigma_1^2 = -9$ and $\sigma_1^2 = -32$ dB onwards for the SN and RN transmit powers, respectively. Equivalently, it can be remarked in the three lower subplots that at high noise power, allocating all the power to the best subchannel is energy efficient; in better channel condition (when σ_1^2 decreases), optimal EE is obtained by sharing the power between subchannels, i.e. breakpoint at $\sigma_1^2 = 12$, $\sigma_1^2 = 8$ and $\sigma_1^2 = 2$ dB for the second, third and fourth subchannels on the three lower subplots. These results confirm our premise that allocating power to all the M subchannels is EE-optimal when the aggregate channel gain-to-noise ratio is high. Moreover, the results regarding p_m

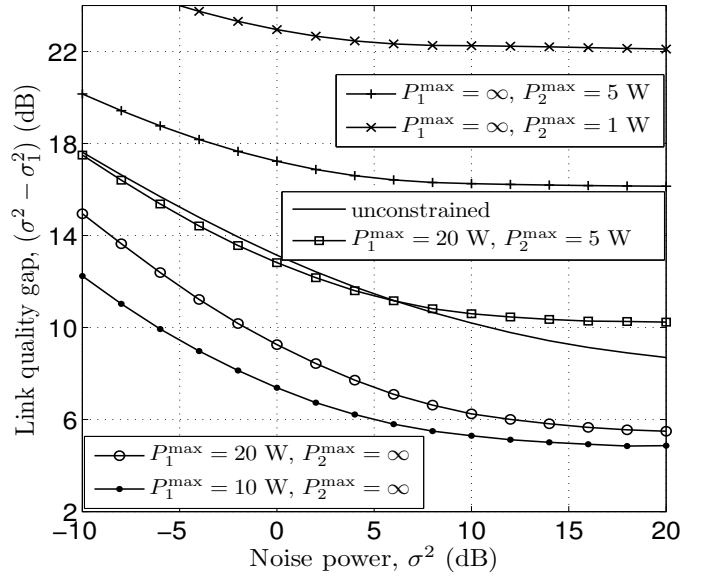


Fig. 5: Minimum relay channel gain improvement for MIMO-AF to be more energy efficient than MIMO for various scenarios.

(in the second subplot) confirms that equal aggregate power allocation is the most energy efficient power allocation in the unconstrained scenario since all the p_m^* converge towards $W E_b^* / \ln(2)$. Finally, the graphs show the great accuracy of our asymptotic expressions for the EE-optimal SN and RN per-subchannel transmit powers in (38).

B. Application: EE comparison of MIMO-AF with MIMO systems

As an application for our algorithms, we compare the EE of MIMO and MIMO-AF systems with CSI, and analyze in which scenarios MIMO-AF can be more energy efficient than MIMO systems.

1) *MIMO-AF vs. MIMO EE insights*: Firstly, MIMO-AF incurs extra power consumption in comparison with a MIMO system due to the usage of a relay and the two-phase communication. Hence, P_0 in the energy-per-bit formulation of the MIMO system in (15) is always lower than \bar{P}_c in (19a). Secondly, it can easily be proved from (12) that the per-subchannel aggregate rate \mathcal{C}_m can be bounded as follows

$$[\min\{\mathcal{C}_{1,m}, \mathcal{C}_{2,m}\} - 1]^+ \leq \mathcal{C}_m \leq \min\{\mathcal{C}_{1,m}, \mathcal{C}_{2,m}\}.$$

In other words, \mathcal{C}_m can only be as good as the worst of the two links' rate. Consequently, these two disadvantages make MIMO-AF always less energy-efficient than MIMO if the channel gain-to-noise ratio of both systems are equivalent, i.e. B_m in (15) is equal to A_m in (19a).

In Fig. 5, we depict the minimum channel gain improvement, averaged over 10000 runs, that the usage of a relay must achieve for MIMO-AF to be more energy efficient than MIMO as a function of the MIMO noise power, σ^2 , in MIMO Rayleigh fading when $M = 8$, $\sigma_1^2 = \sigma_2^2$. Given that regardless of the configuration this minimum channel gain improvement is positive (> 5 dB), it confirms that the usage of a relay must

TABLE II: Simulation parameter values

Parameters (Unit)		Values
f_c (GHz)		2
W (MHz)		10
N_0 (dBm/Hz)	RN	-170.5
	UE	-165.2
G_{TxRx} (dBi)	BS to UE	14
	BS to RN	14
	RN to UE	5

provide channel gain improvement for MIMO-AF to be more energy-efficient than MIMO systems. In the unconstrained scenario MIMO-AF must improve the quality of each link by at least 10 dB, i.e. about one order of magnitude. Whereas less channel improvement is required from MIMO-AF when the SN transmit power is constrained; in this case, MIMO achieves a suboptimal EE, as it is explained in Section III-D, whereas, MIMO-AF can fine-tune the power at the RN for improving the EE. However, the graph also indicates that MIMO-AF capability to improve the EE is largely diminished when the RN transmit power is constrained; indeed, the second hop acts as a bottleneck in this case.

2) *MIMO-AF vs. MIMO EE results*: In a realistic system, the channel gain improvement translates into pathloss improvement. Assuming a simple distant-dependent pathloss model such that $\rho_{i,m} = 10^{\Gamma - 10\kappa \log_{10}(d)}$ and knowing that a relay can at best split the SN-DN distance by half for each hop, we can expect a channel gain improvement of 3κ dB by using a relay, where κ is the pathloss exponent, Γ is a constant and d is the distance. Hence, relaying is likely to be more beneficial in terms of EE when the direct channel quality is poor, i.e. for high values of κ . This also echoes the results of Fig. 5, where the minimum channel gain improvement decreases as the direct link quality worsens, i.e. when σ^2 increases.

In order to illustrate this hypothesis, we compare in Figs. 6 and 7, the EE-optimal transmit power, consumed power, sum-rate and energy-per-bit of MIMO-AF and MIMO systems, averaged over 10000 runs, by taking into account both pathloss and small scale (Rayleigh) fading. We also consider practical simulation parameter values, which are reported in Table II, MaBS or Micro BS (MiBS) at the SN, $M = 256$, i.e. $N = 2$ & $K = 128$, and the linear layout of Fig. 1 such that D , αD and $(1-\alpha)D$ are the SN-DN, SN-RN and RN-DN distances, respectively. In both figures, we utilize the following pathloss model between two nodes

$$\rho = 10^{(G_{\text{TxRx}} - \text{PL}(d))/10},$$

where G_{TxRx} is the antenna gain, and $\text{PL}(d) = \text{Pb}_{\text{LOS}}(d) \times \text{PL}_{\text{LOS}}(d) + (1 - \text{Pb}_{\text{LOS}}) \text{PL}_{\text{NLOS}}(d)$ is the distance dependent path-loss function. In addition, Pb_{LOS} is the line-of-sight (LOS) probability, $\text{PL}_{\text{LOS}}(d)$ and $\text{PL}_{\text{NLOS}}(d)$ are the LOS and non-LOS (NLOS) path-loss functions, whose values can be found in Table 33 of [42]. Note that we considered here Pb_{LOS} for the suburban scenario, i.e. scenario 2 in Table 33 of [42].

The total transmit power results in the upper-left corner of Figs. 6 and 7 indicate that the usage of a relay can be beneficial

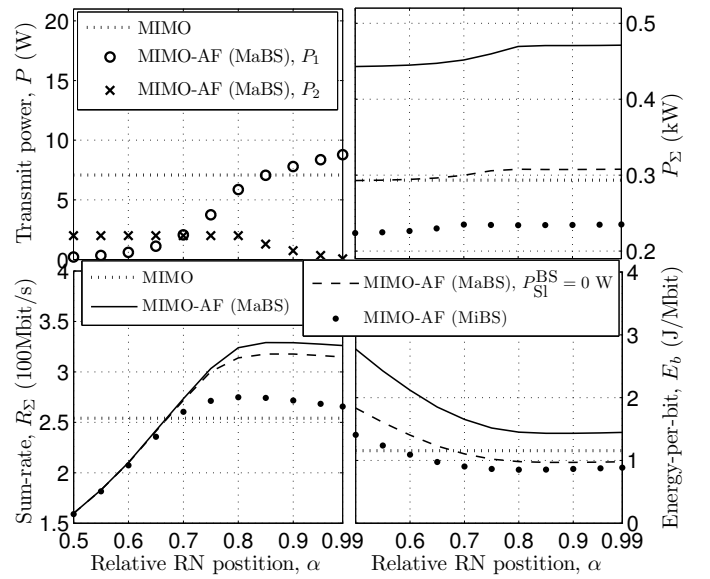


Fig. 6: Comparison of the EE-optimal transmit power, consumed power, sum-rate and energy-per-bit of MIMO-AF against MIMO for practical settings and $D = 0.5$ km.

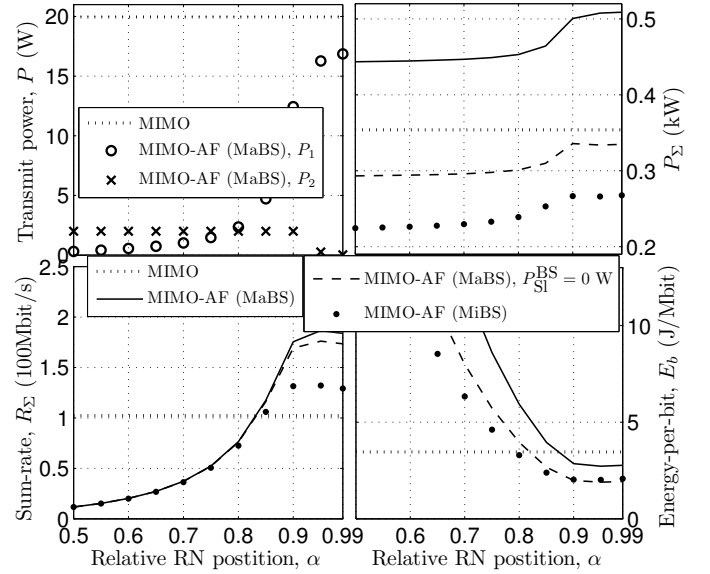


Fig. 7: Comparison of the EE-optimal transmit power, consumed power, sum-rate and energy-per-bit of MIMO-AF against MIMO for practical settings and $D = 2$ km.

for reducing the transmit power since for most RN positions, especially when $D = 2$ km in Fig. 7, the total transmit power consumption of MIMO is greater than the one of MIMO-AF, i.e. $P_1 + P_2$. However, this reduction in transmit power does not translate into reduction in total consumed power. Indeed, P_{Σ} of MIMO-AF is far higher than P_{Σ} of MIMO in the upper-right corner of both figures, because MIMO-AF induces extra overhead power such as the BS sleeping mode power. In terms of sum-rate, the results in the lower-left corner of Figs. 6 and 7 show that MIMO-AF can improve the latter by more than 50% when the RN is close to the DN. Indeed, given that the transmit power of the RN is 20 times lower than that of the MaBS, the EE-optimal transmit power of the RN is constrained when it is far from the DN and, hence, the second hop acts as

bottleneck, as we previously remarked in Fig. 5. The sum-rate improvement translates into an EE improvement in the lower-right corner of Fig. 7 but only when $D = 2$ km. It confirms that relaying is mainly beneficial in terms of EE when the direct channel quality is poor, i.e. when the DN is far from the SN (cell edge user). However, this EE improvement is solely the result of sum-rate improvement and not power reduction. If now we consider that the BS sleeping mode power, $P_{\text{SI}}^{\text{BS}}$, is equal to zero, i.e. the BS is switched off during the second transmission phase, or that a MiBS ($G_{\text{TxRx,BS to RN}} = 7$ dBi, see Table I for power parameter values) is used instead of the MaBS at the SN for the MIMO-AF system, then the usage of MIMO-AF can really be beneficial in terms of EE. This is in line with the fact that the amount of transmit power that is required for being energy efficient decreases as the circuit power decreases in the MIMO system [43]. It can be remarked in the lower-part of Figs. 6 and 7, that some of the extra sum-rate provided by MIMO-AF can be traded-off for reducing the total power consumption when using a MiBS instead of a MaBS at the SN, which in turn, reduces the energy-per-bit consumption. Finally, it is worth noting that the positioning of the relay is an important factor for the MIMO-AF system to be or not to be energy efficient.

V. CONCLUSION

In this paper, a low-complexity energy-efficient joint resource allocation method has been designed for the two-hop MIMO-AF system when considering that full CSI is available at the RN and transmit CSI is available at the SN. We have demonstrated how to simplify the multivariate unconstrained, power and sum-rate constrained EE problems into single or dual variate problems by proving that our EE-based objective function has a unique global minimum and showing its similarity with the single-hop MIMO scenario. Based on this insight, we have derived explicit formulations of the near-optimal energy-per-bit consumption, subchannels' rate and power for all our EE optimization problems of interest and provided algorithms for solving these problems in a low-complexity manner. These explicit formulations have also been utilized for showing that equal aggregate power allocation and full subchannel allocation are the most energy-efficient strategies in the unconstrained and general cases, respectively, when the channel gain-to-noise ratio is high. Simulations have demonstrated in various scenarios that our method is both reliable and accurate when compared to a classic optimization method and the iterative method of [33]. As an application, we have compared the EE-optimal performances of the two-hop MIMO-AF and MIMO systems with CSI. The results have indicated that the usage of a relay must improve the link quality by around one order of magnitude per hop for the two-hop MIMO-AF to be more energy-efficient than the MIMO system, when the relay is mid-way between the SN and DN. Our results have also indicated that the extra fixed power consumption induced by transmitting over two hops disadvantage MIMO-AF over MIMO systems in terms of EE. Reducing this fixed power consumption and placing the relay wisely are two important factors for MIMO-AF to be more

energy efficient than MIMO systems. In the future, we would like to generalize this work for any number of hops and to include the duplexing ratio in the optimization process.

APPENDIX

A. Proof for Proposition 1

Proof: The function E_b in (10) is continuous and twice differentiable such that its gradient and Hessian can be expressed as

$$\nabla E_b(\mathbf{C}) = \frac{\nabla P_{\Sigma}(\mathbf{C})R_{\Sigma}(\mathbf{C}) - \nabla R_{\Sigma}(\mathbf{C})P_{\Sigma}(\mathbf{C})}{R_{\Sigma}(\mathbf{C})^2} \quad \text{and} \quad (39a)$$

$$\begin{aligned} \nabla^2 E_b(\mathbf{C}) &= \frac{\nabla^2 P_{\Sigma}(\mathbf{C})R_{\Sigma}(\mathbf{C}) - \nabla^2 R_{\Sigma}(\mathbf{C})P_{\Sigma}(\mathbf{C})}{R_{\Sigma}(\mathbf{C})^2} \\ &+ \frac{\nabla R_{\Sigma}(\mathbf{C})^T \nabla E_b(\mathbf{C}) + \nabla E_b(\mathbf{C})^T \nabla R_{\Sigma}(\mathbf{C})}{R_{\Sigma}(\mathbf{C})}, \end{aligned} \quad (39b)$$

respectively, where $\{\cdot\}^T$ is the transpose operator. In addition,

$$\nabla P_{\Sigma}(\mathbf{C}) = \ln(2)[A_{1,1}2^{C_{1,1}}, \dots, A_{2,1}2^{C_{2,1}}, \dots, A_{2,M}2^{C_{2,M}}], \quad (40a)$$

$$\nabla^2 P_{\Sigma}(\mathbf{C}) = \ln(2) \text{diag}\{\nabla P_{\Sigma}(\mathbf{C})\}, \quad (40b)$$

where $\text{diag}\{\cdot\}$ is the diagonal operator, and

$$\begin{aligned} \nabla R_{\Sigma}(\mathbf{C}) &= W \left[\frac{2^{C_{2,1}} - 1}{2^{C_{1,1}} + 2^{C_{2,1}} - 1}, \dots, \frac{2^{C_{2,M}} - 1}{2^{C_{1,M}} + 2^{C_{2,M}} - 1} \right. \\ &\left. , \frac{2^{C_{1,1}} - 1}{2^{C_{1,1}} + 2^{C_{2,1}} - 1}, \dots, \frac{2^{C_{1,M}} - 1}{2^{C_{1,M}} + 2^{C_{2,M}} - 1} \right], \end{aligned} \quad (41a)$$

$$\begin{aligned} \{\nabla^2 R_{\Sigma}(\mathbf{C})\}_{\{i,m\},\{j,l\}} &= \frac{\partial^2 R_{\Sigma}(\mathbf{C})}{\partial C_{i,m} \partial C_{j,l}} \\ &= \begin{cases} -W \ln(2) \frac{2^{C_{i,m}} (2^{C_{i,m}} - 1)}{(2^{C_{1,m}} + 2^{C_{2,m}} - 1)^2} & \text{if } j = i \text{ and } l = m \\ W \ln(2) \frac{2^{C_{i,m} + C_{i,m}}}{(2^{C_{1,m}} + 2^{C_{2,m}} - 1)^2} & \text{if } j = \bar{i} \text{ and } l = m \\ 0 & \text{otherwise.} \end{cases} \end{aligned} \quad (41b)$$

According to (39b), $\nabla E_b(\mathbf{C})\mathbf{z}^T = 0$ implies that $R_{\Sigma}(\mathbf{C})^2 \mathbf{z} \nabla^2 E_b(\mathbf{C}) \mathbf{z}^T = \mathbf{z} \nabla^2 P_{\Sigma}(\mathbf{C}) \mathbf{z}^T R_{\Sigma}(\mathbf{C}) - \mathbf{z} \nabla^2 R_{\Sigma}(\mathbf{C}) \mathbf{z}^T P_{\Sigma}(\mathbf{C})$, or equivalently with (40b) that $R_{\Sigma}(\mathbf{C})^2 \mathbf{z} \nabla^2 E_b(\mathbf{C}) \mathbf{z}^T = \ln(2) \mathbf{z} \cdot (\nabla P_{\Sigma}(\mathbf{C}) R_{\Sigma}(\mathbf{C}) \mathbf{z}^T) - \mathbf{z} \nabla^2 R_{\Sigma}(\mathbf{C}) \mathbf{z}^T P_{\Sigma}(\mathbf{C})$, where \cdot denotes the dot product. In addition, since $\nabla P_{\Sigma}(\mathbf{C}) R_{\Sigma}(\mathbf{C}) \mathbf{z}^T = \nabla R_{\Sigma}(\mathbf{C}) P_{\Sigma}(\mathbf{C}) \mathbf{z}^T$ when $\nabla E_b(\mathbf{C}) \mathbf{z}^T = 0$, $\mathbf{z} \nabla^2 E_b(\mathbf{C}) \mathbf{z}^T$ can be re-expressed as $\mathbf{z} \nabla^2 E_b(\mathbf{C}) \mathbf{z}^T =$

$$\begin{aligned} &\frac{\ln(2) P_{\Sigma}(\mathbf{C})}{R_{\Sigma}(\mathbf{C})^2} \left(\mathbf{z} \cdot (\nabla R_{\Sigma}(\mathbf{C}) \mathbf{z}^T) - \frac{\mathbf{z} \nabla^2 R_{\Sigma}(\mathbf{C}) \mathbf{z}^T}{\ln(2)} \right) \\ &\frac{W \ln(2) P_{\Sigma}(\mathbf{C})}{R_{\Sigma}(\mathbf{C})^2} \sum_{m=1}^M H_m(\mathbf{C}), \end{aligned} \quad (42)$$

where

$$\begin{aligned} H_m(\mathbf{C}) &= 2^{C_{1,m} + C_{2,m}} (z_{1,m} - z_{2,m})^2 + \sum_{i=1}^2 z_{i,m}^2 \left[(2^{C_{i,m}} - 1)^2 \right. \\ &\left. + 2^{C_{i,m}} (2^{C_{i,m}} - 1) \right]. \end{aligned}$$

Since $H_m(\mathbf{C}) \geq 0$ when $C_{i,m} \geq 0$, for any $i \in \{1, 2\}$ and $m \in \mathcal{M} = \{1, \dots, M\}$, we can conclude that $\nabla E_b(\mathbf{C})\mathbf{z}^T = 0 \Rightarrow \mathbf{z} \nabla^2 E_b(\mathbf{C}) \mathbf{z}^T \geq 0$ for any $\mathbf{C} \succeq 0$ such that E_b is quasiconvex

over its domain, i.e. unimodal, according to (3.21) of [41]. In other words, E_b can have several local minima, but it has a global minimum value. Note that any local minima, which are not global, are not strict minima [44].

Let \mathbf{C}^* be a stationary point of E_b , accordingly, $\nabla E_b(\mathbf{C} = \mathbf{C}^*) = 0$. Moreover, we know from (39a) that if $\nabla E_b(\mathbf{C})\mathbf{z}^T = 0$ then $E_b(\mathbf{C}) = \frac{\nabla P_\Sigma(\mathbf{C})\mathbf{z}^T}{\nabla R_\Sigma(\mathbf{C})\mathbf{z}^T}$ such that $E_b(\mathbf{C} + \mathbf{z}) - E_b(\mathbf{C}) =$

$$\frac{\nabla P_\Sigma(\mathbf{C})(2^{\mathbf{z}} - 1)^T}{\ln(2)R_\Sigma(\mathbf{C} + \mathbf{z})} - \frac{[R_\Sigma(\mathbf{C} + \mathbf{z}) - R_\Sigma(\mathbf{C})] \nabla P_\Sigma(\mathbf{C})\mathbf{z}^T}{R_\Sigma(\mathbf{C} + \mathbf{z})\nabla R_\Sigma(\mathbf{C})\mathbf{z}^T}. \quad (43)$$

In addition, let $F : \mathbf{X} \in \mathbb{R}^{2M} \mapsto \mathbb{R}$ and $\|\mathbf{z}\| \ll 1$, then the gradient of F is similar to

$$\nabla F(\mathbf{X})\mathbf{z}^T \simeq F(\mathbf{X} + \mathbf{z}) - F(\mathbf{X}). \quad (44)$$

Given that $\nabla P_\Sigma(\mathbf{C})(2^{\mathbf{z}} - 1)^T > \ln(2)\nabla P_\Sigma(\mathbf{C})\mathbf{z}^T$, for $\mathbf{z} \neq \mathbf{0}$, it implies with (43) and (44) that $E_b(\mathbf{C}^* + \mathbf{z}) > E_b(\mathbf{C}^*)$. Consequently, any stationary point is a strict local minima and, hence, according to theorem 6.2 of [44], a strict global minima of E_b . ■

B. Proof for Proposition 2

Proof: On the one hand, by inserting (12) into equations (3) and (6), the latter can be re-expressed as

$$R_\Sigma(\mathbf{C}) = W \sum_{m=1}^M C_m, \quad \text{and} \quad (45a)$$

$$P_i(\mathbf{C}) = \Delta_i^{-1} \sum_{m=1}^M A_{i,m} \left[(2^{C_m} - 1) + 2^{C_m} \frac{2^{C_{i,m}} (2^{C_{i,m}} - 1)}{2^{C_{1,m} + C_{2,m}}} \right], \quad (45b)$$

respectively. On the other hand, according to (39a) and (29) as well as (34), solving $\nabla E_b(\mathbf{C}^*) = \mathbf{0}$ and $\nabla \mathcal{L}(\mathbf{C}^*, \hat{\mu}_i^*) = \mathbf{0}$ as well as $\nabla \mathcal{L}(\mathbf{C}^*, \hat{\mu}_1^*, \hat{\mu}_2^*) = \mathbf{0}$ in the unconstrained and power constrained scenarios yield $E_b^* = E_b(\mathbf{C}^*) =$

$$\frac{\partial P_\Sigma(\mathbf{C}^*)}{\partial C_{i,m}} \left[\frac{\partial R_\Sigma(\mathbf{C}^*)}{\partial C_{i,m}} \right]^{-1} = \frac{\partial P_\Sigma(\mathbf{C}^*)}{\partial C_{i,m}} \left[\frac{\partial R_\Sigma(\mathbf{C}^*)}{\partial C_{i,m}} \right]^{-1}, \quad (46a)$$

$$\mu_i^* \frac{\partial P_\Sigma(\mathbf{C}^*)}{\partial C_{i,m}} \left[\frac{\partial R_\Sigma(\mathbf{C}^*)}{\partial C_{i,m}} \right]^{-1} = \mu_i^* \frac{\partial P_\Sigma(\mathbf{C}^*)}{\partial C_{i,m}} \left[\frac{\partial R_\Sigma(\mathbf{C}^*)}{\partial C_{i,m}} \right]^{-1}, \quad (46b)$$

respectively, for any $i \in \{1, 2\}$ and $m \in \mathcal{M}^*$, where $\mu_i^* = \hat{\mu}_i^* R_\Sigma(\mathbf{C}^*)$. Note that solving $\nabla \mathcal{L}(\mathbf{C}^*, \nu^*) = \mathbf{0}$ in (26) also yields (46a), but where E_b^* is replaced by ν^* in the left side of (46a). Note also that $\mu_i^* = 1$ in (46b) for the single power constraint case. Thus, according to (46), the following relation holds for all the optimization problems discussed in this paper

$$\mu_1^* \frac{\partial R_\Sigma(\mathbf{C}^*)}{\partial C_{2,m}} \frac{\partial P_\Sigma(\mathbf{C}^*)}{\partial C_{1,m}} = \mu_2^* \frac{\partial R_\Sigma(\mathbf{C}^*)}{\partial C_{1,m}} \frac{\partial P_\Sigma(\mathbf{C}^*)}{\partial C_{2,m}}, \quad (47)$$

where $\mu_1^* = \mu_2^* = 1$ in the unconstrained as well as sum-rate constrained problems, and $\mu_1^* = 1$ or $\mu_2^* = 1$ in the single power constrained problem. In turn, it implies with (47) that any $C_{1,m}$ and $C_{2,m}$ can be related as follows

$$\mu_1^* A_{1,m} 2^{C_{1,m}} (2^{C_{1,m}} - 1) = \mu_2^* A_{2,m} 2^{C_{2,m}} (2^{C_{2,m}} - 1) \quad (48)$$

when $C_{i,m} = C_{i,m}^*$, for any $i \in \{1, 2\}$ and $m \in \mathcal{M}$, such that $C_{1,m}^* = 0 \Leftrightarrow C_{2,m}^* = 0$. Moreover, $A_{i,m} 2^{C_{i,m}} (2^{C_{i,m}} - 1) =$

$$\sqrt{\frac{\mu_i^*}{\mu_i^*}} \sqrt{A_{1,m} A_{2,m} 2^{C_{1,m} + C_{2,m}} (2^{C_{1,m}} - 1) (2^{C_{2,m}} - 1)}. \quad (49)$$

Substituting $A_{i,m} 2^{C_{i,m}} (2^{C_{i,m}} - 1)$ in (45b) with (49) and since $\frac{(2^{C_{1,m}} - 1)(2^{C_{2,m}} - 1)}{2^{C_{1,m} + C_{2,m}}} = 1 - \frac{(2^{C_{1,m} + C_{2,m}} - 1)}{2^{C_{1,m} + C_{2,m}}} = 1 - 2^{-C_m}$, equation (45b) can then be solely expressed as a function of C_m such that

$$P_i(\mathbf{C}) = \Delta_i^{-1} \sum_{m=1}^M A_{i,m} (2^{C_m} - 1) + \sqrt{\frac{A_{1,m} A_{2,m}}{(\mu_i^*)^{-1} \mu_i^*}} \sqrt{2^{C_m} (2^{C_m} - 1)}. \quad (50)$$

Equation (11) is finally obtained by substituting the numerator and denominator of (10) with (50) and (45a), respectively. ■

C. Proof for Proposition 3

Proof: Similar to (46), solving $\nabla E_b(\mathbf{C}^*) = \mathbf{0}$, $\nabla \mathcal{L}(\mathbf{C}^*, \nu^*) = \mathbf{0}$, $\nabla \mathcal{L}(\mathbf{C}^*, \hat{\mu}_i^*) = \mathbf{0}$ and $\nabla \mathcal{L}(\mathbf{C}^*, \hat{\mu}_1^*, \hat{\mu}_2^*) = \mathbf{0}$ in the unconstrained, sum-rate constrained as well as single and dual power constrained scenarios with respect to C_m yield

$$E_b^* = \left(\mu_1^* \Delta_1 \frac{\partial P_1(\mathbf{C}^*)}{\partial C_m} + \mu_2^* \Delta_2 \frac{\partial P_2(\mathbf{C}^*)}{\partial C_m} \right) \left[\frac{\partial R_\Sigma(\mathbf{C}^*)}{\partial C_m} \right]^{-1}, \quad (51)$$

where $\mu_1^* = \mu_2^* = 1$ in the unconstrained as well as sum-rate constrained cases, and $\mu_1^* = 1$ or $\mu_2^* = 1$ in the single power constrained case. Note that E_b^* is replaced by ν^* in the sum-rate constrained case. In addition, $\frac{\partial R_\Sigma(\mathbf{C})}{\partial C_m} = W$ and $\frac{\partial P_i(\mathbf{C})}{\partial C_m} =$

$$\ln(2) \Delta_i^{-1} 2^{C_m} \left[A_{i,m} + \sqrt{\frac{\mu_i^* A_{1,m} A_{2,m}}{4\mu_i^*}} \frac{(2^{C_m+1} - 1)}{\sqrt{2^{C_m} (2^{C_m} - 1)}} \right],$$

according to (45a) and (50), respectively. By inserting these results into (51), equation (16) can then be obtained. ■

ACKNOWLEDGMENT

The author wishes to thank his beloved Wife for her support, and dedicates this work to his late Grandmother.

REFERENCES

- [1] H. Zhang et al., "Energy efficiency in communications," *IEEE Commun. Mag.*, vol. 48, no. 11, pp. 48–79, Nov. 2010.
- [2] —, "Energy efficiency in communications: part II," *IEEE Commun. Mag.*, vol. 49, no. 6, pp. 28–87, Jun. 2011.
- [3] —, "Energy efficiency in communications: part III," *IEEE Commun. Mag.*, vol. 49, no. 8, pp. 52–109, Aug. 2011.
- [4] K. Lahiri, A. Raghunathan, S. Dey, and D. Panigrahi, "Battery-driven System Design: A New Frontier in Low Power Design," in *Proc. Intl. Conf. on VLSI Design*, Bangalore, India, Jan. 2002, pp. 261–267.
- [5] H. M. Kwon and T. G. Birdsall, "Channel Capacity in Bits per Joule," *IEEE J. Ocean. Eng.*, vol. OE-11, no. 1, pp. 97–99, Jan. 1986.
- [6] S. Cui, A. J. Goldsmith, and A. Bahai, "Energy-Efficiency of MIMO and Cooperative MIMO Techniques in Sensor Networks," *IEEE J. Sel. Areas Commun.*, vol. 22, no. 6, pp. 1089–1098, Aug. 2004.
- [7] L. M. Correia, D. Zeller, O. Blume, D. Ferling, Y. Jading, I. Godór, G. Auer, and L. V. D. Perre, "Challenges and Enabling Technologies for Energy Aware Mobile Radio Networks," *IEEE Commun. Mag.*, vol. 48, no. 11, pp. 66–72, Nov. 2010.
- [8] G. Auer et al., "How Much Energy is Needed to Run a Wireless Network?" *IEEE Wireless Commun.*, vol. 18, no. 5, pp. 40–49, Oct. 2011.

- [9] A. Sendonaris, E. Erkip, and B. Aazhang, "User Cooperation Diversity Part I & II- System Description / Implementation Aspects and Performance Analysis," *IEEE Trans. Commun.*, vol. 51, no. 11, pp. 1927–1948, Nov. 2003.
- [10] M. Janani, A. Hedayat, T. E. Hunter, and A. Nosratinia, "Coded Cooperation in Wireless Communications: Space-Time Transmission and Iterative Decoding," *IEEE Trans. Signal Process.*, vol. 52, no. 2, pp. 362–371, Feb. 2004.
- [11] A. Nosratinia, T. E. Hunter, and A. Hedayat, "Cooperative communication in wireless networks," *IEEE Commun. Mag.*, vol. 42, no. 10, pp. 74–80, Oct. 2004.
- [12] J. N. Laneman, D. N. C. Tse, and G. W. Wornell, "Cooperative Diversity in Wireless Networks: Efficient Protocols and Outage Behavior," *IEEE Trans. Inf. Theory*, vol. 50, no. 12, pp. 3062–3080, Dec. 2004.
- [13] "Reconfigurable OFDMA-based Cooperative Networks Enabled by Agile SpecTrum Use (ROCKET)," ICT-215282 FP7 STREP project, Tech. Rep., 2008-2009. [Online]. Available: <http://www.ict-rocket.eu>
- [14] Y. Fan and J. Thompson, "MIMO Configurations for Relay Channels: Theory and Practice," *IEEE Trans. Wireless Commun.*, vol. 6, no. 5, pp. 1774–1786, May 2007.
- [15] O. Muñoz-Medina, J. Vidal, and A. Agustín, "Linear Transceiver Design in Nonregenerative Relays with Channel State Information," *IEEE Trans. Signal Process.*, vol. 55, no. 6, pp. 2593–2604, Jun. 2007.
- [16] I. Hammerström and A. Wittneben, "Power Allocation Schemes for Amplify-and-Forward MIMO-OFDM Relay Links," *IEEE Trans. Wireless Commun.*, vol. 6, no. 8, pp. 2798–2802, Aug. 2007.
- [17] C. B. Chae, T. Tang, R. W. Health, and S. Cho, "MIMO Relaying with Linear Processing for Multi-user Transmission in Fixed Relay Networks," *IEEE Trans. Inf. Theory*, vol. 56, no. 2, pp. 727–738, Feb. 2008.
- [18] C. Li, X. Wang, L. Yang, and W.-P. Zhu, "A Joint Source and Relay Power Allocation Scheme for a Class of MIMO Relay Systems," *IEEE Trans. Signal Process.*, vol. 57, no. 12, pp. 4852–4860, Dec. 2009.
- [19] Y. Yu and Y. Hua, "Power allocation for a MIMO relay system with multiple-antenna users," *IEEE Trans. Signal Process.*, vol. 58, no. 5, pp. 2823–2835, May 2010.
- [20] C. Li, X. Wang, L. Yang, and W.-P. Zhu, "Joint source-and-relay power allocation in multiple-input multiple-output amplify-and-forward relay systems: a non-convex problem and its solution," *IET Signal Processing*, vol. 5, no. 6, pp. 612–622, Jun. 2011.
- [21] R. G. Gallager, *Information Theory and Reliable Communication*. John Wiley & Sons, Inc., 1968.
- [22] D. N. C. Tse and S. V. Hanly, "Multiaccess fading channels. I. Polymatroid structure, optimal resource allocation and throughput capacities," *IEEE Trans. Inf. Theory*, vol. 44, no. 7, pp. 2796–2815, Nov. 1998.
- [23] F. Meshkati, H. V. Poor, S. C. Schwartz, and N. B. Mandayam, "An Energy-Efficient Approach to Power Control and Receiver Design in Wireless Networks," *IEEE Trans. Commun.*, vol. 5, no. 1, pp. 3306–3315, Nov. 2006.
- [24] G. Miao, N. Himayat, and G. Y. Li, "Energy-Efficient Link Adaptation in Frequency-Selective Channels," *IEEE Trans. Commun.*, vol. 58, no. 2, pp. 545–554, Feb. 2010.
- [25] C. Isheden and G. P. Fettweis, "Energy-Efficient Multi-Carrier Link Adaptation with Sum Rate-Dependent Circuit Power," in *Proc. IEEE Globecom*, Miami, USA, Dec. 2010.
- [26] Z. Chong and E. Jorswieck, "Analytical Foundation for Energy Efficiency Optimisation in Cellular Networks with Elastic Traffic," in *Proc. MOBILIGHT 2011*, Bilbao, Spain, May 2011.
- [27] F. Héliot, M. A. Imran, and R. Tafazolli, "Energy-efficiency based resource allocation for the orthogonal multi-user channel," in *Proc. IEEE VTC-Fall*, Québec city, Canada, Sep. 2012.
- [28] Y. Yao, X. Cai, and G. B. Giannakis, "On Energy Efficiency and Optimum Resource Allocation of Relay Transmissions in the Low-power Regime," *IEEE Trans. Wireless Commun.*, vol. 4, no. 6, pp. 2917–2927, Nov. 2005.
- [29] H. Yu, H. Qin, Y. Li, Y. Zhao, X. Xu, and J. Wang, "Energy-efficient power allocation for non-regenerative OFDM relay links," *Science China Information Sciences*, vol. 56, no. 2, pp. 1–8, Feb. 2013.
- [30] C. Sun and C. Yang, "Energy efficiency analysis of one-way and two-way relay systems," *EURASIP J. Wirel. Commun. and Netw.*, vol. 46, no. 2, Feb. 2012.
- [31] K. T. K. Cheung, S. Yang, and L. Hanzo, "Maximizing energy-efficiency in multi-relay OFDMA cellular networks," in *Proc. IEEE Globecom Workshops (GC Wkshps)*, Atlanta, USA, Dec. 2013.
- [32] A. Zappone, Z. Chong, E. A. Jorswieck, and S. Buzzi, "Energy-Aware Competitive Power Control in Relay-Assisted Interference Wireless Networks," *IEEE Trans. Wireless Commun.*, vol. 12, no. 4, pp. 1860–1871, Apr. 2013.
- [33] P. Cao, Z. Chong, Z. K. M. Ho, and E. Jorswieck, "Energy-Efficient Power Allocation for Amplify-and-Forward MIMO Relay Channel," in *Proc. IEEE CAMAD*, Barcelona, Spain, Oct. 2012.
- [34] R. A. Horn and C. R. Johnson, *Matrix Analysis*. Cambridge, UK: Cambridge Univ. Press, 1985.
- [35] Y. Rong and Y. Hua, "Optimality of diagonalization of multi-hop MIMO relays," *IEEE Trans. Wireless Commun.*, vol. 8, no. 12, pp. 6068–6077, Dec. 2009.
- [36] A. Fehske, P. Marsch, and G. Fettweis, "Bit per Joule Efficiency of Cooperating Base Stations in Cellular Networks," in *Proc. IEEE Globecom Workshops (GC Wkshps)*, Miami, USA, Dec. 2010.
- [37] F. Héliot et al., "D3.2: Green Network Technologies," INFISO-ICT-247733 EARTH (Energy Aware Radio and NeTwork Technologies), Tech. Rep., Jan. 2012.
- [38] Y. Qi, F. Héliot, and M. A. Imran, *Green Communications and Networking: Chapter 3: Green Relay Techniques in Cellular Systems*. CRC press, Dec. 2012.
- [39] S. Verdú, "Spectral Efficiency in the Wideband Regime," *IEEE Trans. Inf. Theory*, vol. 48, no. 6, pp. 1319–1343, Jun. 2002.
- [40] R. M. Corless, G. H. Gonnet, D. E. G. Hare, D. J. Jeffrey, and D. E. Knuth, "On the LambertW Function," *Adv. Comput. Math.*, vol. 5, pp. 329–359, 1996.
- [41] S. Boyd and L. Vandenberghe, *Convex Optimization*. Cambridge, UK: Cambridge Univ. Press, 2004.
- [42] A. Ambrosy et al., "D2.2: Definition and Parameterization of Reference Systems and Scenarios," INFISO-ICT-247733 EARTH (Energy Aware Radio and NeTwork Technologies), Tech. Rep., Jun. 2010.
- [43] F. Héliot, M. A. Imran, and R. Tafazolli, "Energy-efficient power allocation for point-to-point MIMO systems over the Rayleigh fading channel," *IEEE Wireless Commun. Lett.*, no. 4, pp. 304–307, Aug. 2012.
- [44] M. Avriel, *Nonlinear Programming: Analysis and Methods*. New-York, Dover Publications, Sep. 2003.



Fabien Héliot (S'05-M'07) received the M.Sc. degree in Telecommunications from the Institut Supérieur de l'Electronique et du Numérique (ISEN), Toulon, France, and the Ph.D. degree in Mobile Telecommunications from King's College London, in 2002 and 2006, respectively. He is currently a Lecturer at the Centre for Communication Systems Research (CCSR) of the University of Surrey. He has been actively involved in European Commission funded projects such as FIREWORKS, ROCKET, SMART-Net projects and more recently in the award-winning EARTH project. He is currently involved in the LexNet project, a project investigating human exposure to electromagnetic fields induced by wireless telecommunication networks. His main research interests are energy efficiency, cooperative communication, MIMO, and radio resource management. He received an Exemplary Reviewer Award from IEEE COMMUNICATIONS LETTERS in 2011.